



# Extraction and Characterization of Chitosan from Snail Shells (*Achatina fulica*)

S. Tertsegha <sup>1\*</sup> , P.I. Akubor <sup>1</sup>, A.A. Iordekighir <sup>2</sup>, K. Christopher <sup>3</sup>, O.O. Okike <sup>2</sup>

1. Department of Food Science and Technology, University of Mkar, Benue State.

2. Nigerian Stored Products Research Institute, Mile 4, Ikwere Road, Rumueme, P.M.B. 5063, Port-Harcourt, Nigeria.

3. Nigerian Stored Products Research Institute, 2 Batawa Close, Hadeja Road, Kano, Nigeria.

## HIGHLIGHTS

- Snail shells is good sources of chitosan.
- Utilization of a locally available and underexploited resource (snail shells), contributing to waste reduction.
- Development of novel bioactive materials with potential applications in food preservation, pharmaceuticals, and medical devices.
- Thiocyanate which is notable for renal toxicity was found in the chitosan.

## Article type

Original article

## Keywords

*Lissachatina fulica*

Chitin

Chitosan

Snails

Spectroscopy, Fourier Transform

Infrared

## Article history

Received: 24 Feb 2024

Revised: 10 May 2024

Accept: 27 Aug 2024

## Acronyms and abbreviations

DD=Degree of Deacetylation

EDS=Electron Dispersive

Spectroscopy

FT-IR=Fourier Transform Infrared

spectroscopy

SEM=Scanning Electron

Microscope

## ABSTRACT

**Background:** Chitosan due to biodegradable and non-toxic characteristics has versatile applications. Extraction and characterization of Chitosan from Snail Shells In January, 2023 *Achatina fulica* was performed.

**Methods:** A chemical process involving demineralization and deproteinization was utilized to extract 2000g Chitin from *Achatina fulica* shells. To produce chitosan, the chitin was subjected to deacetylation. The chitosan was subsequently characterized using Fourier Transform Infrared spectroscopy, X-ray diffraction, and Scanning Electron Microscopy. The physicochemical characteristics and mineral compositions were investigated and the data were analyzed using the Statistical Package for Social Sciences (SPSS) software version 20.0.

**Results:** The chitosan obtained from the process was 75%. It exhibited a Degree Of Deacetylation of 82.31%, a molecular weight of  $2.65 \times 10^5$  g/mol, an intrinsic viscosity of 1,007.2 mg/g, and a solubility of 70%. The pH value of chitosan in acetic acid solution was recorded at 6.38, with a solubility of 70%. The proximate analysis revealed moisture, ash, fat, protein, crude fiber, and carbohydrate contents of 0.32, 0.72, 2.01, 0.13, 0.15, and 96.67%, respectively. The mineral analysis revealed sodium, potassium, calcium, magnesium, phosphorus, iron, and zinc concentrations of 32.10, 21.80, 721, 288.60, 123.75, 41.77, and 8.48 mg/g, respectively. X-ray diffraction analysis identified the region characterized by the presence of calcite and calcium phosphate, indicating residual minerals in the extracted chitosan, which contribute to its crystalline structure. Fourier Transform Infrared spectroscopy demonstrated functional groups such as amino and hydroxyl groups, whereas Scanning Electron Microscopy reported an irregular particle size with rough surfaces and a microfibrillar crystalline structure.

**Conclusion:** The current investigation has the potential to promote the sustainable use of a locally abundant yet underutilized resource, assisting in waste reduction and creation of innovative bioactive materials which could be applied in food preservation, pharmaceuticals, and medical devices.

© 2024, Shahid Sadoughi University of Medical Sciences. This is an open access article under the Creative Commons Attribution 4.0 International License.

\* Corresponding author (S. Tertsegha)

✉ E-mail: tertseghasandra@gmail.com

ORCID ID: <https://orcid.org/0009-0001-3220-5911>

**To cite:** Tertsegha S., Akubor P.I., Iordekighir A.A., Christopher K., Okike O.O. (2024). Extraction and characterization of chitosan from snail shells (*Achatina fulica*). *Journal of Food Quality and Hazards Control*. 11: 186-196.

## Introduction

Chitosan is a linear polysaccharide formed from deacetylated chitin, consisting of  $\beta$ -(1 $\rightarrow$ 4)-linked 2-amino-2-deoxy-D-glucose units. It serves as a major component of fungal cell walls, the exoskeletons of arthropods and insects, and other naturally occurring indigestible oligosaccharides. As one of the most abundant organic substances in nature, chitosan is second only to cellulose (Adekanmi et al., 2020). By eliminating the acetyl groups ( $\text{CH}_3\text{-CO}$ ) from chitin molecules, chitosan can be produced with free amino groups. As the acetamide groups ( $\text{CH}_3\text{CO-NH}$ ) in chitin are replaced with amino groups ( $-\text{NH}_2$ ) in chitosan, chitosan is the deacetylated version of chitin (Sultana et al., 2020).

De Queiroz-Antonino et al. (2017) reported that chitosan is non-toxic, biocompatible, and biodegradable. Its potential to chemically bind with fats, lipids, and bile acids is due to its positive ionic charge (Parvin et al., 2018). As a consequence, chitin and chitosan polymers have garnered increasing interest as potential polymeric materials for applications in the food, chemical, and pharmaceutical industries. Chatterjee et al. (2021) estimated that there are approximately 200 potential and common uses for chitin, chitosan, and their derivatives, including applications in food processing, cosmetics, biomedicine, biocatalysis, and wastewater treatment. Other uses include the purification and immobilization of enzymes, the treatment of wastewater, and the development of new food additives with thickening, binding, gelling, and stabilizing qualities (Martín-Diana et al., 2009). Research have proven that chitosan has antibacterial and antifungal activities (Sayari et al., 2016), which makes it interesting as a new natural antimicrobial compound in response to the growing demands for safe and healthy foods, using natural preservatives.

Snail flesh is consumed in large quantities due to its low cholesterol and high protein content. Snail meat is becoming increasingly popular in Nigerian and African eateries, as well as elsewhere. However, consuming snails produces numerous snail shells, which are subsequently discarded into the environment. Despite being biodegradable, these wastes decompose slowly. Over time, this case results in accumulation, an unpleasant stench, and the presence of rats, flies, and other insects that contaminate the environment. An economically viable source of chitin and chitosan is snail shell. Therefore, the extraction and characterization of the chitosan from the shells of Giant African snails (*Achatina fulica*) will lessen environmental pollution and increase the chitosan's worth in the food sector. Therefore, the study aims to extract and characterize chitosan from Giant African snail (*A. fulica*), with potential applications in food preservation and various biomedical purposes.

## Materials and methods

### Materials

Snail shells (*A. fulica*) weighing 2,500 g utilized in this research were purchased from the Gboko Main market, Benue State, Nigeria in January, 2023. Sodium hydroxide (NaOH 97% purity) from Fizmerk Company, India, nitric acid ( $\text{HNO}_3$  99% purity; Fizmerk Company, India), hydrochloric acid (HCl 97%) from May and Baker Ltd., Dagenham England, and acetic acid (99.8%) from May and Baker Ltd., Nigeria. Reagents were diluted to the appropriate concentrations required for the analytical procedures with deionized water.

### Extraction of chitosan

Chitosan was prepared according to the method described by Chawla et al. (2014). Initially, the snail shells were cleaned of loose tissue, washed thoroughly with distilled water, and dried in a hot air oven (Binder FD 260, Germany) at 60 °C for 24 h. The dried shells were then crushed using a mortar and pestle, ground into a fine powder, and sieved through a 250  $\mu\text{m}$  sieve.

For demineralization, 400 g of the snail shell powder was weighed using an analytical balance and added to 4% HCl (1.3 N) in a ratio of 1:14 g/ml (w/v). This mixture was vigorously shaken and maintained at ambient temperature (32 °C) for 24 h. Afterward, the mixture was thoroughly washed with distilled water to achieve neutrality and sieved through a 250  $\mu\text{m}$  sieve. The residue was subsequently washed with deionized water and oven-dried in a tray dryer at 40 °C for 24 h.

For deproteinization, the demineralized residue (400 g) was treated with 5% NaOH (1.25 N) at a ratio of 1:12 g/ml (w/v), with constant stirring at 90 °C for 2 h to remove the proteins. The mixture was sieved through a 250  $\mu\text{m}$  sieve and filtered under vacuum. The filtrate was washed with distilled water for 30 min until it reached a neutral pH (pH=7). The deproteinized residue was then oven-dried at 60 °C for 24 h.

### Production of chitosan from chitin

Chitosan was prepared according to the method described by Chawla et al. (2014). The extracted chitin (2,000 g) with a particle size of 40  $\mu\text{m}$  was transferred to a ceramic mortar. A 50% (w/v) NaOH solution (20 L) was added to the chitin and mixed thoroughly. The ceramic mortar was then centered on a heater and the mixture was heated at 1,400 W for 8 h. Once heated, the mixture was filtered and the residue was rinsed with distilled water until a neutral pH was reached. The residue was then dried in a hot air oven at 40 °C to a constant weight and subsequently stored in high density polyethylene bags for further analysis.

### Determination of proximate composition of chitosan

The proximate composition of the chitosan was considered to evaluate its moisture, ash, protein, and fiber contents. To measure moisture content, the chitosan samples were dried at 60 °C using an oven to a constant weight, and the moisture content was calculated based on the weight loss. To determine the ash content, the samples were incinerated at 555 °C in a Muffle furnace (SX series, China) and then weighed. Fiber and protein contents were analyzed according to the standard procedures specified by AOAC (2019).

### Determination of mineral composition of chitosan

The mineral composition of the chitosan, including sodium (Na), phosphorus (P), iron (Fe), zinc (Zn), magnesium (Mg), calcium (Ca), and potassium (K), was analyzed using Atomic Absorption Spectrometry (AAS; Shimadzu, 210VGP, USA) and a flame photometer (LTCS05, China) according to AOAC (2019) guidelines. For analysis, 5 g of the sample was weighed into a crucible and ashed in a muffle furnace at 500 °C for 2 h. The ashed sample was then treated with 10 cm<sup>3</sup> of HNO<sub>3</sub> (6 M), stirred until a uniform solution was obtained, and subsequently filtered. The resulting solution was diluted with distilled water. Standard curves for each metal were prepared to quantify the elements using the AAS and flame photometer.

### Evaluation of physicochemical properties of chitosan

#### -Degree of Deacetylation (DD)

The DD of the chitosan sample was determined with regard to the method outlined by Chawla et al. (2014). The deacetylation was achieved by adding 100 ml of 50% NaOH to the sample, which was then boiled at 100 °C for 2 h on a hot plate. Following boiling process, the sample was allowed to cool at room temperature for 30 min. It was thoroughly washed with 50% NaOH and filtered to isolate the solid material, which was chitosan. The chitosan was then remained uncovered and dried in an oven at 120 °C for 24 h. This treatment aimed to produce chitosan with a high DD value (>75%). The DD of the chitosan was measured using a Fourier Transform Infrared spectroscopy (FT-IR; Shimadzu FT-IR-8400, USA) instrument operating within a frequency range of 400-4,000 1/cm. The DD was calculated using the following equation:

$$DD = 100 - \left( \frac{A_{1,655}}{A_{3,450}} \times \frac{100}{1.33} \right)$$

where;  $A_{1,655}$  and  $A_{3,450}$  were the absorbances at 1,655 1/cm of the amide-I band indicating the N-acetyl group content and 3,450 1/cm for the hydroxyl band (used as an internal standard to correct film thickness), respectively. The factor 1.33 corresponds to the value of the ratio of  $A_{1,655}/A_{3,450}$  for completely acetylated chitosan, indicating a linear

relationship between the N-acetyl group content and the absorbance of the amide-I band.

#### -Determination of viscosity and molecular weight

The molecular weight of the chitosan sample was measured by dissolving 1% chitosan (w/v) in 1% glacial acetic acid (Fizmerk Company, India). The intrinsic viscosity ( $\mu$ ) of the solution was measured using an Ubbelohde glass capillary viscometer (HK, China), based on the method described by De Queiroz Antonino et al. (2017). The molecular weight of chitosan was calculated using the Mark-Houwink equation, which correlates intrinsic viscosity to molecular weight with the following empirical viscometric constants:

$$\mu = JM^b$$

$$J = 1.81 \times 10^3 \text{ cm}^3/\text{g}$$

$$b = 0.93 \text{ for chitosan}$$

$$\mu = \text{intrinsic viscosity (ml/g)}$$

$$M = \text{molecular weight (g/mol)}$$

#### -pH of chitosan

The pH of the sample with various treatments was obtained using a digital pH meter (Beckman, USA) equipped with an electrode, following the AOAC (2019) method.

#### Structural analysis

The X-ray diffraction analysis of the samples was accomplished using a Malvern PANalytical X' Pert PRO MPD X-ray diffraction system (United Kingdom). The samples were prepared and located on a sample holder, and X-ray beams were directed through them. Intensity measurements were recorded at Bragg's 2 $\theta$  angles to determine the crystallinity of the chitosan samples. FT-IR was utilized to identify structural differences in the chitosan samples by analyzing their functional groups. Electron Dispersive Spectroscopy (EDS; Oxford Instruments X-Max 50, UK) was employed alongside Scanning Electron Microscopy (SEM; JEOL 6400, Japan) to analyze the elemental composition of the chitosan samples by detecting characteristic X-rays emitted during electron beam irradiation and to visualize the morphology of the chitosan samples. The samples were thinly coated with gold, placed on a sample holder, and micrographs were captured as outlined by Adekanmi et al. (2020).

#### Statistical analysis

Data were analyzed using SPSS statistics (version 20.0). Descriptive statistics were reported as mean  $\pm$  Standard Deviation (SD) for all the variables.

## Results

### Physicochemical properties of chitosan

### -Proximate composition of chitosan

Table 2 displays the proximate composition of chitosan. The result proves that carbohydrates have the highest percentage of 96.67% whereas the rest of the parameters have less than 1%. However, crude fat and crude fibre are 2.01 and 2.25%, respectively.

### Mineral composition of chitosan

The mineral composition of chitosan is presented in Table 3. The result manifested various concentrations of Ca, Na, K, Fe, Mg, P, and Zn. Ca has the highest concentration (721 mg/ml) among all the tested minerals, followed by Mg with 288 mg/ml. The rest of the tested minerals have values below 45 mg/ml, with the exception of P which has 123 mg/ml.

### FT-IR spectroscopy analysis of chitosan

The result of the FT-IR analysis is presented in Figure 1 and reveals spectral features corresponding to essential functional groups. The overall functional groups identified from the FT-IR analysis of the chitosan sample are the hydroxyl, aldehyde, amine, thiocyanate, and lactone groups.

### SEM

The morphology of the extracted chitosan sample at different resolutions is presented in Figure 2 with categories A, B, and C. The result revealed that the particles are polygonal in shape with category A of 100  $\mu\text{m}$  being more conspicuous. However, the surface of category C of 300  $\mu\text{m}$  appears rough and amorphous, reflecting the semi-crystalline nature of the chitosan.

### X-ray diffraction of chitosan

To ascertain the nature of the extracted chitosan, X-ray diffraction analysis was performed and the diffraction profile is presented in Figure 3. The profile is characterized by very broad peaks at  $2\theta=10^\circ$  and  $2\theta=20^\circ$  and sharp peaks at  $2\theta=27^\circ$ ,  $2\theta=40^\circ$ ,  $2\theta=50^\circ$ ,  $2\theta=66^\circ$ ,  $2\theta=74^\circ$ . The broad peaks at  $2\theta=10^\circ$  and  $2\theta=20^\circ$  amorphous nature of the chitosan. On the other hand, the sharp peaks at  $2\theta=27^\circ$ ,  $2\theta=40^\circ$ ,  $2\theta=50^\circ$ ,  $2\theta=66^\circ$ , and

$2\theta=74^\circ$  indicates highly ordered crystalline regions within the chitosan sample. The combination of the broad and sharp peaks is suggestive of the semi-crystalline nature of the chitosan.

### -EDS

The EDS is illustrated in Figure 4. The EDS analysis presents the different peaks for various elements as contained in the chitosan sample. Ca and K have the largest peaks in comparison with others.

**Table 1:** Physicochemical properties of chitosan

Parameter	Chitosan
Yield (%)	75
Fixed carbon (%)	56.99
DD (%)	82.31
Molecular weight (g/mol)	$2.65 \times 10^5$
Intrinsic viscosity (ml/g)	1,007.2
Solubility in acetic acid (%)	70
pH	6.38
Total soluble solids ( $^\circ\text{Brix}$ )	ND
Total titratable acidity (%)	ND

DD=Degree of Deacetylation; ND=Not detected

**Table 2:** Proximate composition of chitosan

Parameter	*Composition (%)
Moisture	$0.32 \pm 0.00$
Ash	$0.72 \pm 0.01$
Crude fat	$2.01 \pm 0.00$
Crude protein	$0.13 \pm 0.00$
Crude fibre	$2.25 \pm 0.00$
Carbohydrate	$96.67 \pm 0.49$

\*Values are Means  $\pm$  Standard Deviation (SD) of 3 replications.

**Table 3:** Mineral composition (mg/ml) of chitosan

Parameters	*Concentrations
Sodium (Na)	$32.10 \pm 0.06$
Potassium (K)	$21.80 \pm 0.00$
Calcium (Ca)	$721 \pm 0.70$
Magnesium (Mg)	$288.60 \pm 0.00$
Phosphorus (P)	$123.75 \pm 0.03$
Iron (Fe)	$41.77 \pm 0.00$
Zinc (Zn)	$8.48 \pm 0.01$

\*Values are means  $\pm$  Standard Deviation (SD) of 3 replications.

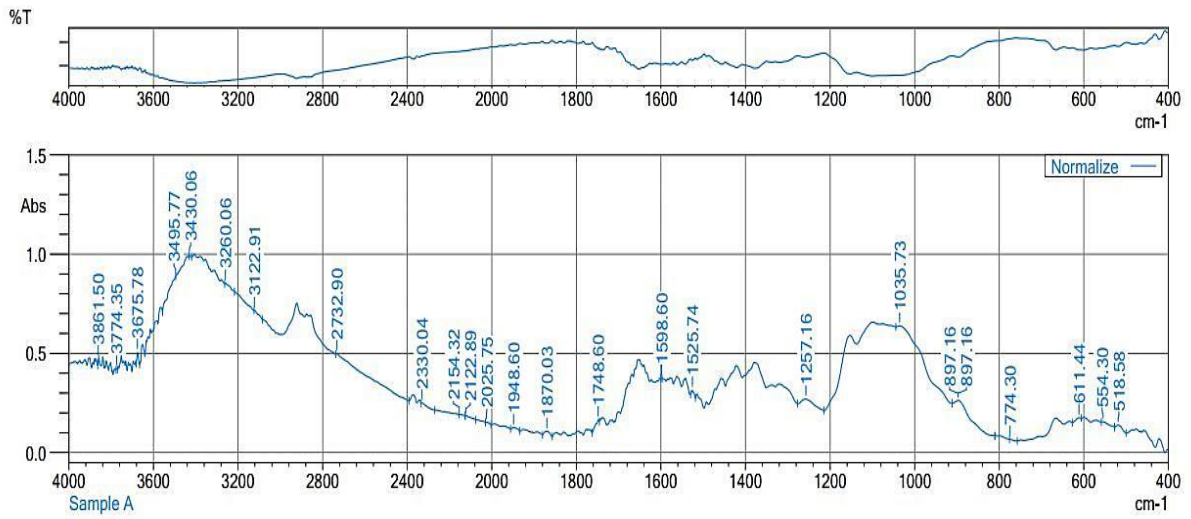


Figure 1: Fourier Transform Infrared (FT-IR) spectroscopy of chitosan

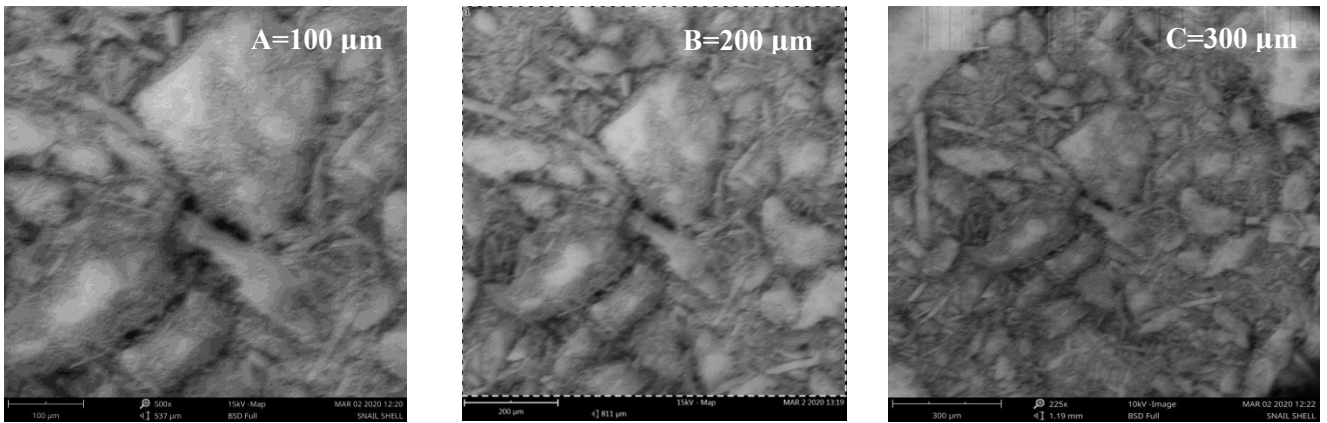


Figure 2: Scanning Electron Microscopy (SEM) Micrograph of extracted chitosan

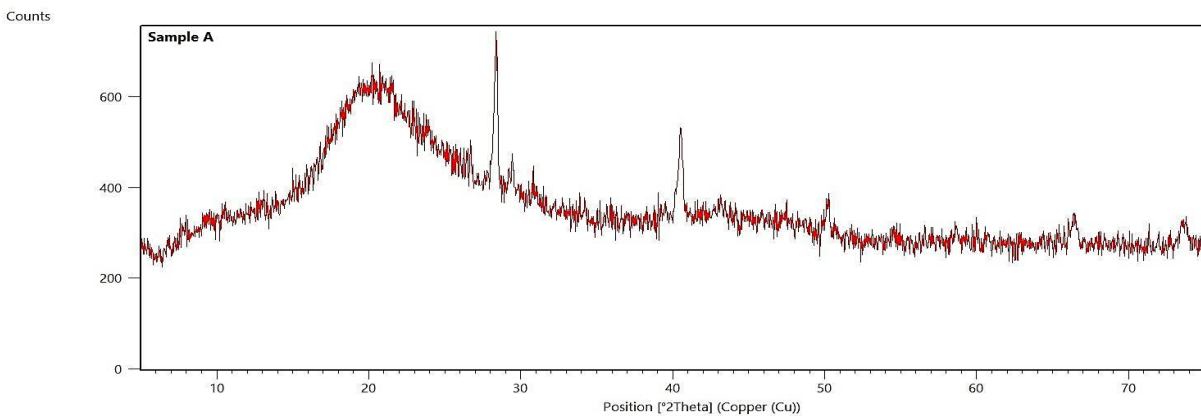
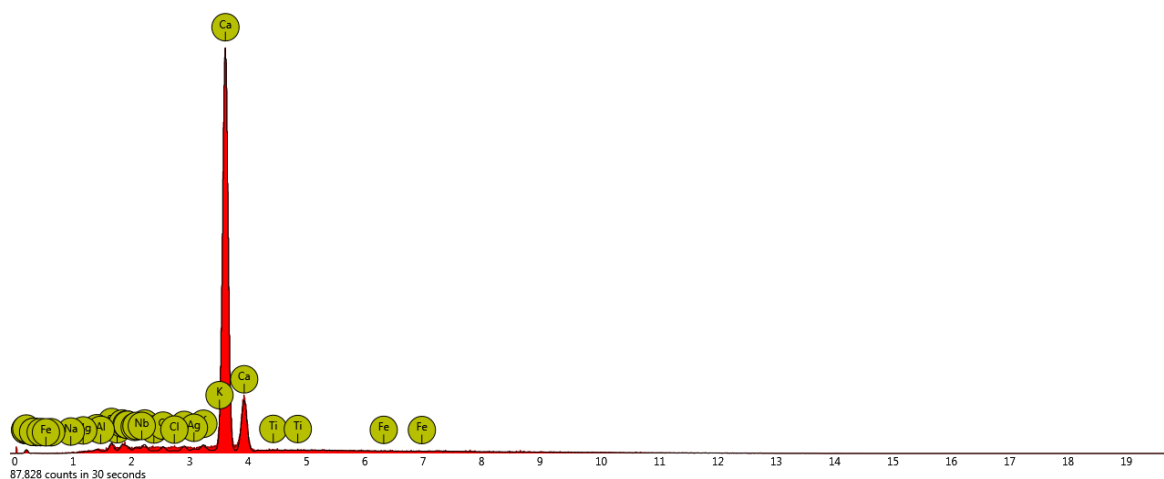


Figure 3: X-ray diffraction of extracted chitosan  
Sample A=Chitosan



**Figure 4:** Electron Dispersive Spectroscopy (EDS)

## Discussion

Chitosan is a high molecular-weight biopolymer, with its molecular weight varying based on the source of the raw material and the preparation method (Tarafdar and Biswas, 2013). Commercial chitosan products typically have a molecular weight in the range of 100,000 to 1,200,000 Da, which is influenced by the preparation process and the grade of the product (Premasudha et al., 2017; Sultana et al., 2020).

Ke et al. (2021) suggested that the ability of chitosan to penetrate cell membranes and exert intracellular antibacterial effects is influenced by its molecular weight. Besides contributing to pathogenesis, surface adhesion (both biotic and abiotic), and the induction of immune responses, the polysaccharides and small amounts of proteins which constitute the complex layers of the cell wall in both bacteria and fungi also provide mechanical strength and act as a barrier against environmental factors (Ke et al., 2021). According to research by Vijayasri and Tiwari (2019), chitosan properties and uses may be affected by degrading mechanisms which alter its molecular weight, such as chemical treatments and radiation.

In Table 1, the molecular weight of chitosan ( $2.65 \times 10^5$  Da) was comparable to the  $8.76 \times 10^5$  and  $5.61 \times 10^5$  Da reported molecular weights of shrimp and crab chitosan, respectively (Sultana et al., 2020). Moreover, according to Hossain and Iqbal (2014), the average molecular weight of shrimp chitosan was  $1.05 \times 10^6$  Da, which was higher than the value in the present study.

The molecular weight of chitosan is determined by its intrinsic viscosity, which also reveals information on the chain length and solution behaviour (Affes et al., 2021). Significant chain interaction is suggested by a high intrinsic viscosity of 1,007.2 ml/g and can impact the behavior of chitosan in solutions and real-world

applications. Similarly, a high viscosity of 720 ml/g was obtained from chitosan extracted, quantified, and characterized from crayfish shells using various sequential methods (Adekanmi et al., 2020). In a variety of solvents, the association between chitosan inherent viscosity and molecular weight has been investigated. According to Min et al. (2023), chitosan from snail shells was more viscous compared to other crustaceans. The intrinsic viscosity of chitosan can be affected by various factors, including the degree of acetylation, pH, and the ionic strength of the solvent (Sikorski et al., 2021; Vijayasri and Tiwari, 2019). Since the pH of 6.38 is in the neutral range, chitosan contains a wide range of potential applications. An identical investigation by Kaewboonruang et al. (2016) reported that the pH range of chitosan extracted from golden apple snail shells through chemical processes was 7.07–7.43, which is slightly higher than the pH value observed in this study. Additionally, chitosan has been explored as a coagulant in brewery wastewater treatment, with findings indicating that it performs optimally at a neutral pH (Khumalo et al., 2023). The neutral pH range is advantageous for the potential use of chitosan in various applications, including drug delivery and wastewater treatment, as its preferred characteristics are enhanced at these pH levels (Sikorski et al., 2021). Moreover, the results uncovered that neither total soluble solids nor total titratable acidity were apparent in the sample. This information is relevant for applications where the presence of solids and acidity can be disruptive, such as in certain food and beverage applications (Sikorski et al., 2021).

The yield of chitosan extracted in this study (Table 1) exceeded the reported yields by Premasudha et al. (2017) for chitosan obtained from shrimp and crab shells, which were 46 and 34%, respectively, as well as the 14% yield from krill reported by Isa et al. (2012). The variation in chitosan yield may be attributed to the environment in which the snails were reared, the snail species, and the

method of chitosan extraction (Sikorski et al., 2021; Vijayasri and Tiwari, 2019).

The fixed carbon content is an essential indicator of the purity of chitosan and, a value of 56.99% suggests a considerable quantity of stabilized carbon in the chitosan structure, which may contribute to its potential applications, particularly in adsorption or catalytic processes (Sikorski et al., 2021). The high fixed carbon content in chitosan implies its potential for use in adsorption and catalytic processes, as supported by the research on chitosan-derived carbon materials and hydrogels (Sikorski et al., 2021).

The solubility of chitosan in acetic acid solution (Table 1) is consistent with the findings of Sultana et al. (2020), who reported a solubility of 70% for crab chitosan. This consistency highlights the solubility of the chitosan in acetic acid solution reported in this study. Sultana et al. (2020) emphasized that solubility is an integral quality characteristic of chitosan, with higher solubility indicating higher-grade chitosan. Dissolving chitosan in organic solvents, alkaline solutions, or water is demanding (Affes et al., 2021). However, the presence of amino groups facilitates chitosan's ability to dissolve in diluted aqueous acid solutions. Furthermore, Premasudha et al. (2017) identified that factors affecting chitosan solubility were attributed to the temperature and duration of deacetylation, alkali concentration, treatments utilized for chitin separation, the ratio of chitin to alkali solution, and particle size. DD was found to influence the solubility of chitosan; for chitosan to be as soluble as intended, at least 85% of its deacetylation needed to be completed (Tarafdar and Biswas, 2013). Chitosan solubility in mild inorganic acid may be due to high proportion of strongly protonated free amino groups, which attract ionic substances more readily than chitin does (Premasudha et al., 2017).

The 82.31% DD recorded in this work is comparable to the 80.12 and 88.46% DD reported by Premasudha et al. (2017) for chitosan derived from shrimp and crab shells, respectively. Identical findings were presented by Hossain and Iqbal (2014), observing an average DD of 80% for shrimp chitosan, with a range of 56-99%. Sultana et al. (2020) estimated DD values of 76 and 65% for shrimp and crab chitosan, respectively. Puvvada et al. (2012) highlighted that DD is a critical feature influencing the chemical and physical characteristics of chitosan, containing its solubility, adsorption, chemical reactivity, covalent bonding, encapsulation, and biodegradability. The proportion of free amino groups in chitosan influencing these properties, is highly determined by the DD, which is affected by the extraction process and source. Factors containing the source of chitin, the concentrations of acid and alkali used, extraction duration, and temperature all impact the extent of deacetylation (Sikorski et al., 2021;

Vijayasri and Tiwari, 2019).

The moisture content of the chitosan extracted from snail shells in this investigation (Table 2) is significantly lower compared to the moisture content reported in other research studies (Isa et al., 2012; Lam et al., 2023). Maintaining a low moisture content assists to extend the shelf life of chitosan. As chitosan is inherently hygroscopic, the quantity of moisture collected during storage affects the chitosan sample's characteristics. The range of acceptable moisture content for chitosan during the application procedure was 5.0-15.0% (Oyekunle and Omoleye, 2019). A critical component of the final product is moisture. Since numerous spoiling organisms cannot survive at low moisture concentrations, it aids to prolong the shelf life of items. To ensure a prolonged shelf life, chitosan must maintain a low moisture content. The reduced moisture content in chitosan assists to prevent spoilage by decreasing enzymatic and microbial activity, thereby inhibiting the growth of spoilage microorganisms (Oladzadabbasabadi et al., 2022).

The ash content of 0.72% for the chitosan in this research is identical to the 0.31% reported for chitosan from shrimp shells but lower than the 2.28% reported for crab shells chitosan (Olafadehan et al., 2021). This result is consistent with the ash contents reported by Sultana et al. (2020), which were 0.28% for crab shell chitosan and 0.31% for shrimp shell chitosan. Ash is an inorganic residue detected in food that reveals the proportion of minerals it contains (Sundalian et al., 2021). A low ash concentration in the chitosan signified that the demineralization stage, which removes calcium carbonate ( $\text{CaCO}_3$ ), had been successfully completed. High-quality chitosan is defined as having an ash value of less than 1% (Sundalian et al., 2021). Therefore, the ash content of the chitosan obtained in this research indicates that it is of high quality.

The protein content of the chitosan in this study (0.13%) was lower than the 3.80 and 3.92% reported by Olafadehan et al. (2021) for chitosan extracted from shrimp and crab shells, respectively. This lower protein content probably due to the effective removal of protein during the deproteinization process, signifying that the chitosan is not a significant source of protein. In addition, the chitosan's fiber content of the chitosan (0.15%) was lower compared to the 8.01 and 8.45% reported by Olafadehan et al. (2021) for chitosan derived from shrimp and crab shells, respectively. Fiber content serves as a reliable indicator of the degree of crystallinity of the extracted polymers, with higher fiber concentrations typically corresponding to increased crystallinity.

In Table 2, the chitosan's fat content of 2.01% was consistent with reports of 2.00 and 2.30% for chitosan samples from shrimp and crab trash, respectively (Olafadehan et al., 2021). Foods high in carbohydrate

levels are excellent sources of energy (Sundalian et al., 2021). Data regarding levels of mineral compounds in the extracted chitosan are illustrated in Table 3. The chitosan had various levels of minerals. The chitosan contained numerous minerals with Ca having the highest mineral content whereas Zn included the lowest quantity. Olafadehan et al. (2021) reported that snail shells contain a variety of mineral compounds, with  $\text{CaCO}_3$  being the predominant component.

The result of the FT-IR analysis is presented in Figure 1 and revealed spectral features corresponding to essential functional groups in the chitosan samples. Broad absorption bands in the range of 3,600 to 3,900  $1/\text{cm}$  represent strong O-H stretching vibrations, suggesting the presence of hydroxyl groups essential for hydrogen bonding. This observation is consistent with the findings of Rajathy et al. (2021) in *Telescopium telescopium*. This feature is in agreement with the nature of the polysaccharides in chitosan, which contains numerous hydroxyl groups contributing to reactivity and solubility (Wang et al., 2020). The detection of the N-H stretching vibration within 3,100 to 3,500  $1/\text{cm}$  confirms the presence of amine groups which are prominent features of chitosan resulting from the deacetylation of chitin. These amine groups are regarded essential for the bioactivity of the polymer, including antimicrobial and biocompatible characteristics (Pham et al., 2021). A prominent band at 1,748.60  $1/\text{cm}$  corresponds to C=O stretching vibrations and manifests the presence of 6-membered lactones and  $\delta$ -lactones. These lactones likely result from the intermolecular reaction of carboxylic acid groups with adjacent hydroxyl or halogen atoms, contributing to the structural complexity and versatility of chitosan's functions (Rosiak et al., 2021). The band around 2,732.90  $1/\text{cm}$  represents a C-H stretching vibration due to aldehyde groups, demonstrating a possible oxidative modification or residual component from the extraction process (Wang et al., 2020). A 2,154.32  $1/\text{cm}$ , which is an S-C $\equiv$ N stretching vibration, is characteristic of thiocyanate. The presence of thiocyanate is an indication of toxicological concern due to its effect on the renal tissue at high dosages (Thillai et al., 2017). The obtained results from this investigation are comparable to the ones reported by Kaewboonruang et al. (2016), characterizing chitosan from golden apple snail shells, with the exception of the residual thiocyanate. This case recommends that detoxification of the chitosan sample prior to application on consumables is crucial. Bands of 1,525.74  $1/\text{cm}$  are within the range of the N-O stretching vibration implying the presence of nitro compounds. According to Noriega et al. (2022), Nitro compounds are noteworthy for their wide spectrum of activities which consist of antineoplastic, antibiotic, antiparasitic, antihypertensive and tranquilizer. In the fingerprint region,

bands at 1,257.16 and 897.16  $1/\text{cm}$  are connected with C-N stretching and out-of-plane C-H bending vibrations, respectively. This appears identical to the observation by Rajathy et al. (2021) in *T. telescopium* and demonstrates molecular interactions and the overall integrity of the chitosan necessary for its functional properties. The band at 1,035.73  $1/\text{cm}$ , representing a substituted urea derivative, supports the strong antimicrobial effects observed in previous in-silico studies (Gündüz et al., 2020). The FT-IR data conclusively confirm the presence of functional groups, containing amino and hydroxyl groups. The results clarify minimal variation in comparison with previous research, with differences probably attributed to the DD and variations in the chitosan synthesis process between different studies (Acosta-Ferreira et al., 2020).

The microfibrillar crystalline structure and irregular particle size with rough surfaces were evident by morphological analysis of the extracted chitosan sample at various resolutions (Figure 2: A, B, and C). Its deformed and disordered microstructure is devoid of apparent pore spaces. Based on Mohan et al. (2019), the strong O-H bonding in the chitosan contributes to its fibrillar shape. This structure is identical to the chitosan modified by Kaewboonruang et al. (2016) from golden apple snails, although their chitosan exhibited smoother surfaces. According to Tavares et al. (2020), despite the high DD observed in the chitosan from this study, the rough surface is attributed to a low DD. In addition, the chitosan displayed well-defined semi-crystalline layers, which may result from the deacetylation of chitin, removing several bonding agents and exposing more structural sheaths in the chitosan, as noted by Adekanmi et al. (2020). Conversely, the semi-crystalline layer could be attributed to cross-linkage between functional groups and Ca ions, which influences its mechanical strength and gel-forming characteristics (Rajeswari et al., 2020). The produced chitosan in this study closely resembles the one reported by Acosta-Ferreira et al. (2020).

The X-ray diffraction profile of the chitosan sample, as illustrated in Figure 3, exhibited a combination of broad and sharp peaks. In particular, the profile featured broad peaks at  $2\theta=10^\circ$  and  $2\theta=20^\circ$ , along with sharp peaks at  $2\theta=27^\circ$ ,  $2\theta=40^\circ$ ,  $2\theta=50^\circ$ ,  $2\theta=66^\circ$ , and  $2\theta=74^\circ$ . The broad peak at  $2\theta=10^\circ$  is associated with the (020) plane, indicating the presence of amorphous regions in the chitosan (Hasan et al., 2022). The breadth of the peak suggests a lack of long-range order, which is characteristic of the less structured, amorphous regions of the polymer (Facchinatto et al., 2020). The broad peak at  $2\theta=20^\circ$  corresponds to the (110) plane, exhibiting the formation of semi-crystalline regions. This may result from intermolecular and intramolecular hydrogen bonding between the hydroxyl and amine groups in the



chitosan sample (Hasan et al., 2022). Moreover, the breadth of this peak implies a significant proportion of disorder, although it is more ordered in comparison with the entirely amorphous regions. This observation aligns with the findings of Idriss et al. (2024), who reported a semi-crystalline structure in pure chitosan derived from natural wood modified with shrimp shell waste, ascribed to the mixture of amorphous and crystalline regions. Conversely, the presence of sharp peaks at  $2\theta=27^\circ$ ,  $40^\circ$ ,  $50^\circ$ ,  $66^\circ$ , and  $74^\circ$  suggests the presence of highly ordered crystalline regions within the chitosan sample. These sharp peaks recommend that certain crystalline domains are well-defined, possibly due to the alignment of polymer chains in specific orientations (Alves et al., 2019). The sharp peak at  $2\theta=27^\circ$  may correspond to highly ordered crystalline structures, reinforcing the entire crystalline nature of the polymer. Furthermore, the peaks at higher angles ( $2\theta=40^\circ$ ,  $2\theta=50^\circ$ ,  $2\theta=66^\circ$ , and  $2\theta=74^\circ$ ) reflect the existence of smaller and more defined crystalline regions within the sample. The combination of broad and sharp peaks in the X-ray diffraction pattern suggests that the chitosan sample possesses a complex structure with both amorphous and crystalline characteristics. The broad peaks signify the presence of disordered, amorphous regions, whereas the sharp peaks refer to the existence of well-ordered crystalline domains (Hasan et al., 2022). This dual nature of chitosan is critical to its functional properties, as the amorphous regions contribute to its solubility and flexibility, while the crystalline regions impart mechanical strength and thermal stability (Rosiak et al., 2021). Enhanced crystallinity, as evidenced by the sharp peaks, can improve the mechanical features of chitosan, causing it more appropriate for applications requiring high strength and stability. On the other hand, the presence of amorphous regions, as denoted by the broad peaks, can enhance the solubility and bioavailability of the polymer, causing it advantageous for biomedical applications like drug delivery and food preservation (Alves et al., 2019).

Figure 4 displays the EDS analysis of the African snail chitosan. The EDS analysis complements the X-ray diffraction results by identifying the elemental composition of the chitosan sample. The EDS spectrum reveals distinct peaks corresponding to the elements present in the sample, with Ca and K being the most prominent peaks. This indicates that Ca and K are the most abundant elements in chitosan, which could be due to their roles in the extraction or modification processes (Kaewboonruang et al., 2016). The presence of significant proportions of Ca and K can affect the properties of chitosan. Ca is noted to interact with chitosan chains, forming cross-links with functional groups such as hydroxyl and carboxyl groups. This

interaction can potentially improve the gel-forming ability and mechanical characteristics of chitosan (Rajeswari et al., 2020). K can contribute to the ionic strength and stability of the chitosan solution, affecting its solubility and bioactivity. Yan et al. (2021) proposed that K ions can enhance the antimicrobial effect by maintaining the solubility and charge distribution in the chitosan, thereby facilitating its interaction with negatively charged microbial cell membranes. Kaewboonruang et al. (2016), reported that the presence of mineral elements may be suggestive of residual impurities during the extraction process. The semi-crystalline nature of the chitosan samples, as evidenced by the broad and sharp peaks in the X-ray diffraction, coupled with the elemental composition revealed by the EDS, highlights the complex and multifunctional nature of the chitosan (Facchinatto et al., 2020).

## Conclusion

The *A. fulica* shell-derived chitosan exhibited a semi-crystalline structure, excellent solubility, a high DD, and a high yield. This is consistent with the structural analysis conducted using FT-IR spectroscopy, EDS, SEM micrograph, and X-ray diffraction. Caution or modification should be considered to obtain chitosan devoid of impurities such as thiocyanate which is of toxicological concern due to its effect on the kidney tissue that is found in the sample. As a result, chitosan from the *A. fulica* snail shell can be used for food preservations and other biomedical uses. Further research could focus on increasing the yield and DD by potentially optimizing factors including the size reduction of chitin, varying reagent concentrations, adjusting reaction times, and increasing the deacetylation temperature, as suggested by the present literature.

## Author contributions

S.T. and A.A.I. designed and performed the work; P.I.A. supervised the research, reviewed the manuscript, and editing; K.C. and O.O.O. accomplished the data analysis and wrote the manuscript as well. All authors read and approved the final manuscript.

## Conflicts of interest

The authors declare that there is no conflict of interest.

## Acknowledgements

The authors are grateful to the Head of the Department of Food Science and Technology, University of Mkar, Benue State, Nigeria, for the permission to use the Departmental laboratory.

## Funding

This research received no specific grant from any funding agency in the public, commercial, or non-profit sectors.

## Ethical considration

Not applicable.

## References

- Acosta-Ferreira S., Castillo O.S., Madera-Santana J.T., Mendoza-García D.A., Núñez-Colín C.A., Grijalva-Verdugo C., Villalerna A.G., Morales-Vargas A.T., Rodríguez-Núñez J.R. (2020). Production and physicochemical characterization of chitosan for the harvesting of wild microalgae consortia. *Biotechnology Reports*. 28: e00554. [DOI: 10.1016/j.btre.2020.e00554]
- Adekanmi A.A., Adekanmi S.A., Adekanmi O.S. (2020). Different processing sequential protocols for extraction, quantification and characterization of chitosan from cray fish. *International Journal of Engineering and Information Systems*. 4: 47-61.
- Affes S., Aranaz I., Acosta N., Heras Á., Nasri M., Maalej H. (2021). Chitosan derivatives-based films as pH-sensitive drug delivery systems with enhanced antioxidant and antibacterial properties. *International Journal of Biological Macromolecules*. 182: 730-742. [DOI: 10.1016/j.ijbiomac.2021.04.014]
- Alves R., Sabadini R.C., Gonçalves T.S., De Camargo A.S.S., Pawlicka A., Silva M.M. (2019). Structural, morphological, thermal and electrochemical characteristics of chitosan: praseodymium triflate based solid polymer electrolytes. *International Journal of Green Energy*. 16: 1602-1610. [DOI: 10.1080/15435075.2019.1677239]
- Association of Official Analytical Chemists (AOAC). (2019). Official methods of analysis of the association of official analytical chemists: official methods of analysis of AOAC international. 21<sup>st</sup> edition. AOAC, Washington, DC.
- Chatterjee S., Hui P.C.-L., Siu W.S., Kan C.-W., Leung P.-C., Wanxue C., Chiou J.-C. (2021). Influence of pH-responsive compounds synthesized from chitosan and hyaluronic acid on dual-responsive (pH/temperature) hydrogel drug delivery systems of Cortex Moutan. *International Journal of Biological Macromolecules*. 168: 163-174. [DOI: 10.1016/j.ijbiomac.2020.12.035]
- Chawla S.P., Kanatt S.R., Sharma A.K. (2014). Chitosan. In: Ramawat K., Mérillon J.M. (Editors). *Polysaccharides*. Springer, Cham, Switzerland. [DOI: 10.1007/978-3-319-03751-6\_13-1]
- De Queiroz Antonino R.S.C.M., Lia Fook B.R.P., De Oliveira Lima V.A., De Farias Rached R.Í., Lima E.P.N., Da Silva Lima R.J., Covas C.A.P., Lia Fook M.V. (2017). Preparation and characterization of chitosan obtained from shells of shrimp (*Litopenaeus vannamei* Boone). *Marine Drugs*. 15: 141. [DOI: 10.3390/md15050141]
- Facchinatto W.M., Dos Santos D.M., Fiamingo A., Bernardes-Filho R., Campana-Filho S.P., De Azevedo E.R., Colnago L.A. (2020). Evaluation of chitosan crystallinity: a high-resolution solid-state NMR spectroscopy approach. *Carbohydrate Polymers*. 250: 116891. [DOI: 10.1016/j.carbpol.2020.116891]
- Gündüz M.G., Uğur S.B., Güney F., Özkul C., Krishna V.S., Kaya S., Sriram D., Doğan Ş.D. (2020). 1,3-Disubstituted urea derivatives: synthesis, antimicrobial activity evaluation and *in silico* studies. *Bioorganic Chemistry*. 102: 104104. [DOI: 10.1016/j.bioorg.2020.104104]
- Hasan S., Boddu V.M., Viswanath D.S., Ghosh T.K. (2022). The structural difference between chitin and chitosan. In: *Chitin and chitosan. Engineering Materials and Processes*. Springer, Cham. pp: 79-102. [DOI: 10.1007/978-3-031-01229-7\_4]
- Hossain M.S., Iqbal A. (2014). Production and characterization of chitosan from shrimp waste. *Journal of the Bangladesh Agricultural University*. 12: 153-160. [DOI: 10.22004/ag.econ.209911]
- Idriss H.O., Seddik N.B., Achache M., Rami S., Zarki Y., Ennamri A., Janoub F., Bouchta D., Chaouket F., Raissouni I. (2024). Shrimp shell waste-modified natural wood and its use as a reservoir of corrosion inhibitor (L-arginine) for brass in 3% NaCl medium: Experimental and theoretical studies. *Journal of Molecular Liquids*. 398: 124330. [DOI: 10.1016/j.molliq.2024.124330]
- Isa M.T., Ameh A.O., Tijjani M., Adama K.K. (2012). Extraction and characterization of chitin and chitosan from Nigerian shrimps. *International Journal of Biological and Chemical Sciences*. 6: 446-453. [DOI: 10.4314/ijbcs.v6i1.40]
- Kaewboonruang S., Phatrabuddha N., Sawangwong P., Pitaksanurat S. (2016). Comparative studies on the extraction of chitin – chitosan from golden apple snail shells at the control field. *Journal of Polymer and Textile Engineering*. 3: 34-41. [DOI: 10.9790/019X-03013441]
- Ke C.-L., Deng F.-S., Chuang C.-Y., Lin C.-H. (2021). Antimicrobial actions and applications of chitosan. *Polymers*. 13: 904. [DOI: 10.3390/polym13060904]
- Khumalo S.M., Bakare B.F., Tetteh E.K., Rathilal S. (2023). Application of response surface methodology on brewery wastewater treatment using chitosan as a coagulant. *Water*. 15: 1176. [DOI: 10.3390/w15061176]
- Lam I.L.J., Mohd Affandy M.A., Nur Aqilah N., Vonnice J.M., Felicia W.X.L., Rovina K. (2023). Physicochemical characterization and antimicrobial analysis of vegetal chitosan extracted from distinct forest fungi species. *Polymers*. 15: 2328. [DOI: 10.3390/polym15102328]
- Martin-Diana A.B., Rico D., Barat J.M., Barry-Ryan C. (2009). Orange juices enriched with chitosan: optimisation for extending the shelf-life. *Innovative Food Science and Emerging Technologies*. 10: 590-600. [DOI: 10.1016/j.ifset.2009.05.003]
- Min H., Zhang K., Guo Z., Chi F., Fu L., Li B., Qiao X., Wang S., Cao S., Wang B., Ma Q. (2023). N-rich chitosan-derived porous carbon materials for efficient CO<sub>2</sub> adsorption and gas separation. *Frontiers in Chemistry*. 11: 1333475. [DOI: 10.3389/fchem.2023.1333475]
- Mohan K., Ravichandran S., Muralisankar T., Uthayakumar V., Chandirasekar R., Rajeevgandhi C., Rajan D.K., Seedeivi P. (2019). Extraction and characterization of chitin from sea snail *Conus inscriptus* (Reeve, 1843). *International Journal of Biological Macromolecules*. 126: 555-560. [DOI: 10.1016/j.ijbiomac.2018.12.241]
- Noriega S., Cardoso-Ortiz J., López-Luna A., Cuevas-Flores

- M.D.R., Flores De La Torre J.A. (2022). The diverse biological activity of recently synthesized nitro compounds. *Pharmaceuticals*. 15: 717. [DOI: 10.3390/ph15060717]
- Oladzadabbasabadi N., Mohammadi Nafchi A., Ariffin F., Jeevani Osadee Wijekoon M.M., Al-Hassan A.A., Dheyab M.A., Ghasemlou M. (2022). Recent advances in extraction, modification, and application of chitosan in packaging industry. *Carbohydrate Polymers*. 277: 118876. [DOI: 10.1016/j.carbpol.2021.118876]
- Olafadehan O.A., Amoo K.O., Ajayi T.O., Bello V.E. (2021). Extraction and characterization of chitin and chitosan from *Callinectes amnicola* and *Penaeus notialis* shell wastes. *Journal of Chemical Engineering and Materials Science*. 12: 1-30. [DOI: 10.5897/JCEMS2020.0353]
- Oyekunle D.T., Omoleye J.A. (2019). New process for synthesizing chitosan from snail shells. *IOP Conference Series: Journal of Physics*. 1299: 012089. [DOI: 10.1088/1742-6596/1299/1/012089]
- Parvin N., Kader M.A., Huque R., Molla M.E., Khan M.A. (2018). Extension of shelf-life of tomato using irradiated chitosan and its physical and biochemical characteristics. *International Letters of Natural Sciences*. 67: 16-23. [DOI: 10.56431/p-75f52p]
- Pham P., Oliver S., Wong E.H.H., Boyer C. (2021). Effect of hydrophilic groups on the bioactivity of antimicrobial polymers. *Polymer Chemistry*. 12: 5689-5703. [DOI: 10.1039/D1PY01075A]
- Premasudha P., Vanathi P., Abirami M. (2017). Extraction and characterization of chitosan from crustacean waste: a constructive waste management approach. *International Journal of Science and Research*. 6: 1194-1198. [DOI: 10.21275/ART20175408]
- Puvvada Y.S., Vankayalapati S., Sukhavasi S. (2012). Extraction of chitin from chitosan from exoskeleton of shrimp for application in the pharmaceutical industry. *International Current Pharmaceutical Journal*. 1: 258-263.
- Rajathy T.J., Srinivasan M., Mohanraj T. (2021). Physicochemical and functional characterization of chitosan from horn snail gastropod *Telescopium telescopium*. *Journal of Applied Pharmaceutical Science*. 11: 052-058. [DOI: 10.7324/JAPS.2021.110207]
- Rajeswari A., Gopi S., Christy E.J.S., Jayaraj K., Pius A. (2020). Current research on the blends of chitosan as new biomaterials. In: Gopi S., Thomas S., Pius A. (Editors). *Handbook of chitin and chitosan*. Elsevier, Amsterdam, Netherlands. pp: 247-283. [DOI: 10.1016/B978-0-12-817970-3.00009-2]
- Rosiak P., Latanska I., Paul P., Sujka W., Kolesinska B. (2021). Modification of alginates to modulate their physico-chemical properties and obtain biomaterials with different functional properties. *Molecules*. 26: 7264. [DOI: 10.3390/molecules26237264]
- Sayari N., Sila A., Abdelmalek B.E., Abdallah R.B., Ellouz-Chaabouni S., Bougateg A., Balti R. (2016). Chitin and chitosan from the Norway lobster by-products: antimicrobial and anti-proliferative activities. *International Journal of Biological Macromolecules*. 87: 163-171. [DOI: 10.1016/j.ijbiomac.2016.02.057]
- Sikorski D., Gzyra-Jagiela K., Draczyński Z. (2021). The kinetics of chitosan degradation in organic acid solutions. *Marine Drugs*. 19: 236. [DOI: 10.3390/md19050236]
- Sultana S., Hossain M.S., Iqbal A. (2020). Comparative characteristics of chitosan extracted from shrimp and crab shell and its application for clarification of pineapple juice. *Journal of the Bangladesh Agricultural University*. 18: 131-137.
- Sundalian M., Husein S.G., Putri N.K.D. (2021). Review: analysis and benefit of shells content of freshwater and land snails from gastropods class. *Biointerface Research in Applied Chemistry*. 12: 508-517. [DOI: 10.33263/BRIAC121.508517]
- Tarafdar A., Biswas G. (2013). Extraction of chitosan from prawn shell wastes and examination of its viable commercial applications. *International Journal of Theoretical and Applied Research Mechanical Engineering*. 2: 17-24.
- Tavares L., Flores E.E.E., Rodrigues R.C., Hertz P.F., Noreña C.P.Z. (2020). Effect of deacetylation degree of chitosan on rheological properties and physical chemical characteristics of genipin-crosslinked chitosan beads. *Food Hydrocolloids*. 106: 105876. [DOI: 10.1016/j.foodhyd.2020.105876]
- Thillai Natarajan S., Kalyanasundaram N., Ravi S. (2017). Extraction and characterization of chitin and chitosan from achatinodes. *Natural Products Chemistry and Research*. 5: 281. [DOI: 10.4172/2329-6836.1000281]
- Vijayarsi K., Tiwari A. (2019). Radiation degraded chitosan: efficiency and investigation of adsorption of arsenic (v) from aqueous solution. *Analytical Chemistry Letters*. 9: 182-195. [DOI: 10.1080/22297928.2019.1608855]
- Wang W., Meng Q., Li Q., Liu J., Zhou M., Jin Z., Zhao K. (2020). Chitosan derivatives and their application in biomedicine. *International Journal of Molecular Sciences*. 21: 487. [DOI: 10.3390/ijms21020487]
- Yan D., Li Y., Liu Y., Li N., Zhang X., Yan C. (2021). Antimicrobial properties of chitosan and chitosan derivatives in the treatment of enteric infections. *Molecules*. 26: 7136. [DOI: 10.3390/molecules26237136]